High-throughput phenotyping of a large tomato collection under water deficit: Combining UAVs' remote sensing with conventional leaf-level physiologic and agronomic measurements

Article *in* Agricultural Water Management · February 2022

DOI: 10.1016/j.agwat.2021.107283

5 authors, including:

Mateu Fullana-Pericàs
University of the Balearic Islands
17 PUBLICATIONS **291** CITATIONS
SEE PROFILE

Miquel Àngel Conesa
University of the Balearic Islands
98 PUBLICATIONS **1,553** CITATIONS
SEE PROFILE

Jorge Gago
University of the Balearic Islands
77 PUBLICATIONS **4,101** CITATIONS
SEE PROFILE

Jeroni Galmés
University of the Balearic Islands
196 PUBLICATIONS **12,459** CITATIONS
SEE PROFILE

Agricultural Water Management 260 (2022) 107283

Contents lists available at ScienceDirect

Agricultural Water Management

journal homepage: www.elsevier.com/locate/agwat

High-throughput phenotyping of a large tomato collection under water deficit: Combining UAVs' remote sensing with conventional leaf-level physiologic and agronomic measurements

Mateu Fullana-Pericàs *, Miquel À. Conesa, Jorge Gago, Miquel Ribas-Carbó, Jeroni Galmés

Research Group on Plant Biology under Mediterranean Conditions-INAGEA. Universitat de les Illes Balears, Balearic Islands, Spain

ARTICLE INFO

Handling Editor Enrique Fernández

Keywords:
Field phenotyping
Fruit quality
Landraces
NDVI
Photosynthesis
Remote sensing
WUE

ABSTRACT

Field high-throughput phenotyping (HTPP) studies are highly needed to study water use efficiency (WUE), stress tolerance capacities, yield and quality in tomato to improve crop breeding strategies and adapt them to the climatic change scenario. In this study, UAV remote sensing is tested by comparison with leaf-level physiologic and agronomic measurements in a collection including 91 tomato genotypes. These genotypes include long shelf-life (LSL) and non-LSL (CON) Mediterranean landraces, cultivated under well-watered (WW, covering 100% crop evapotranspiration demands) and water deficit (WD, irrigation stopped one month after plantlet transplantation to field) conditions. Aerial remote sensing (including multispectral imaging), leaf gas-exchange, leaf carbon isotope composition ($\delta^{13}C$), fruit production and quality measurements, including total soluble solids and acidity, were performed. Differences between CON and LSL genotypes were observed in leaf-level physiologic and remote sensing measurements under both WW and WD conditions, while for agronomic measurements differences were only found for quality traits under WW conditions. Significant relationships were detected between remote sensing and leaf-level physiologic and agronomic measurements when considering all genotypes and treatments. However, different regressions were described for CON and LSL genotypes, mainly due their different physiologic behavior and response to WD. For instance, for the same NDVI value LSL genotypes showed near 30% lower A_N and half g_s than CON, and therefore higher intrinsic water use efficiency (WUE_i). Also, tomato fruit quality was approached through remote sensing measurements, being correlated with multispectral indices. In conclusion, this study shows how remote sensing can help to optimize tomato physiologic and agronomic phenotyping processes. However, it also points out that the inclusion of genotypes with a different water use efficiency behavior and response to WD lead to a large scattering in the relationships between remote sensing and physiologic and agronomic traits and prevents to obtention of reliable models.

1. Introduction

Global climate models based into the climatic change predict increases in the annual mean temperature for the next decades, especially in the summer season (Battisti and Naylor, 2009). In the Mediterranean basin, temperature increase will be accompanied by reductions in the rainfall from 25% to 50% (Giorgi and Lionello, 2008; Hertig and Tramblay, 2017; Raymond et al., 2019). Considering this scenario, improving water use efficiency (WUE) and stress tolerance in crops becomes a challenge to meet global food demands at the lowest agricultural water consumption. The increase of plants WUE is usually related to lower leaf transpiration rates, leading to increased leaf temperature, and results in lower photosynthetic rates, plant growth and yield (Condon et al., 2002; Eamus, 1991; Medrano et al., 2015). Thus, there is an urgent need to characterize the performance of large numbers of crop genotypes under field conditions in order to detect those with increased WUE and drought tolerance, but still sustaining acceptable commercial fruit production and quality (Mickelbart et al., 2015). For this purpose, the use of high-throughput phenotyping (HTPP) technologies, usually based on remote sensing, allow to obtain detailed, valuable and non-invasive information suitable to be related and to complement plant-level measurements in order to drive novel strategies in crop improvement towards climate change (Araus et al., 2018).

The use of remote sensing technology mounted on unmanned aerial

---

* Corresponding author.
E-mail address: m.fullana@uib.cat (M. Fullana-Pericàs).

https://doi.org/10.1016/j.agwat.2021.107283
Received 7 May 2021; Received in revised form 14 October 2021; Accepted 19 October 2021

vehicles (UAVs) to monitor crop fields has revolutionized field phenotyping in the last years (Adão et al., 2017; Araus et al., 2018; Gago et al., 2015; Salas Fernandez et al., 2017). Those UAVs employed to monitor vegetation are usually equipped with red-green-blue (RGB) and multi-spectral cameras to collect data about vegetation coverage, plant size and height, and allow to measure vegetation indices (VIs) based on canopy reflectance and thermography (Gago et al., 2015; Goel et al., 2003; Zarco-Tejada et al., 2012). The VIs have been used for plant phenotyping to assess the plant physiological status under abiotic stresses in different herbaceous crops including wheat, maize and tomato (Babar et al., 2006; Cairns et al., 2012; Comar et al., 2012; Gianquinto et al., 2011; Padilla et al., 2015; Zarco-Tejada et al., 2012), and also woody crops as olive or grapevine (Calderón et al., 2015; Caruso et al., 2019; Zarco-Tejada et al., 2005). Among the VIs, the normalized difference vegetation index (NDVI) is probably the most commonly used to estimate biomass production, plant vigor, stress levels, yield, and even as a proxy to photosynthesis (Fortes et al., 2015, 2014; Gamon et al., 2015; Steltzer and Welker, 2006; Virlet et al., 2015). UAVs HTPP technology can overcome some of the previous spatial and temporal limitations intrinsic to the traditional leaf-level physiologic measurements. However, there are still information gaps regarding the relationship between the data acquired through plant-truth eco-physiologic techniques and high-throughput UAV phenotyping. Therefore, further integrative approaches are required to improve our understanding of the different genotypes' performance at real field conditions (Araus et al., 2018; Gago et al., 2015).

For instance, leaf gas-exchange parameters as net CO_2 assimilation rate (A_N), stomatal conductance (g_s) and their ratio, known as intrinsic water use efficiency (WUE_i, as A_N/g_s), are widely used as dynamic references for plant performance, physiological stress status, growth dynamics and fruit production, and have been related to aerial remote sensing data (Araus et al., 2018; Flexas and Medrano, 2002; Gago et al., 2017; Zarco-Tejada et al., 2016). Also, carbon isotope composition in leaf tissues ($\delta^{13}C$) has been defined as an integrative physiological stress and WUE indicator (Dhanapal et al., 2015; Farquhar and Richards, 1984), providing information at different levels and time scales (Flanagan and Farquhar, 2014; Tambussi et al., 2007). Despite the correlation between $\delta^{13}C$ and WUE_i is widely defined in literature, their relationship may be affected by the interaction between environment and genotypic variability (Condon, 2004). Although both leaf gas-exchange traits and $\delta^{13}C$ provide highly valuable information to evaluate crop breeding performance, their measurement is time consuming and economically expensive when screening a large number of plants. Additionally, both are mostly focused at leaf rather than plant-level, limiting a wide overview of the crop physiology, and are difficult to implement in field trials at which, added to large plant numbers, parameters should be measured within a narrow timescale and/or in a periodic way along the season (Araus and Cairns, 2014; Gago et al., 2015).

Tomato (*Solanum lycopersicum* L.) is one of the most produced vegetables worldwide and its production has been almost doubled in the last 20 years, from 1000 million to 1900 million tones (FAO, 2021). Despite tomato crop is widely distributed and adapted to an important range of climates (Cuartero and Fernández-Muñoz, 1999), it is mainly cultivated in temperate regions, particularly the Mediterranean basin. At open-field, tomato is a spring-summer high water-demanding crop, requiring more than 3 L per plant and day at maturity (Harmanto et al., 2005). Considering the predicted climate change scenario, it becomes essential to explore the tomato genotypic variability to find the most resilient genotypes under stress conditions, becoming valuable genetic resources to improve WUE minimizing reductions in fruit production and quality under harsh conditions. In this regard, tomato crop is a notorious target for improvement given its worldwide importance and given it has become the model species for fleshy fruit corps (Giovannoni, 2006; Klee and Giovannoni, 2011; The Tomato Genome Consortium, 2012).

Within tomato, most drought-resilient genotypes have been described among local landraces in the Mediterranean basin, due to their selection over centuries under Mediterranean summer conditions (Bota et al., 2014; Guida et al., 2017; Ochogavía et al., 2011; Patanè et al., 2016). Among those, several long shelf-life (LSL) landraces have improved drought tolerance as compared to modern genotypes, and some of their adaptive mechanisms allowing to increase WUE have already been described (Conesa et al., 2020; Fullana-Pericàs et al., 2019; Galmés et al., 2013, 2011; Guida et al., 2017; Tranchida-Lombardo et al., 2018). The LSL phenotype, characterized by an extended fruit post-harvest conservation, exists in several West-Mediterranean landraces like the 'de Ramellet' tomato from the Balearic Islands (Bota et al., 2014; Conesa et al., 2014), the 'de Penjar' tomato from the Eastern Iberian Peninsula (Casals et al., 2012), and in some Italian (Sacco et al., 2017; Sinesio et al., 2007) and Greek landraces (Terzopoulos and Bebeli, 2010) (extended review of LSL landraces distribution and traits can be found in Conesa et al., 2020).

Previous studies used remote sensing and HTPP in tomato to increase phenotyping precision and detect early effects of abiotic stresses, suggesting their implementation in large collections (Daniel et al., 2016; Janni et al., 2019; Johansen et al., 2020, 2019; Ramos-Infante et al., 2019; Vuong et al., 2020). In this study, the physiologic and agronomic performance of 91 tomato genotypes under well-watered and deficit irrigation conditions was assessed using high-throughput UAV phenotyping technologies, and it was validated by comparing with conventional leaf-level physiologic measurements at plant level. The screened genotypes included 68 Western-Mediterranean LSL landraces, and 23 non-LSL landraces and modern inbreeds of very diverse origin and fruit types; most with evidence for improved tolerance to open-field summer cultivation conditions. We hypothesized a differential genotype performance regarding productivity and drought adaptation that should emerge at canopy and leaf levels. Thus, our objectives were: (1) to assess the use of remote sensing measurements to physiologically and agronomically phenotype a large and variable tomato collection and its response to water deficit, and (2) to investigate if the relationships between remote sensing and leaf-level physiologic measurements and agronomic traits are different depending on the tomato genotype or group.

2. Material and methods

2.1. Plant material

Ninety-one tomato genotypes (*Solanum lycopersicum* L.) were evaluated in this study. Two genotype groups were stablished, namely control genotypes (CON, 23 genotypes) and long shelf-life landraces (LSL, 68 genotypes). The CON group included non-LSL landraces from the Mediterranean basin and the M82 and OH8245 genotypes, which were included as two non-Mediterranean control genotypes. The LSL group included genotypes from different Western-Mediterranean regions, covering most of the variability. Genotype codes and seed providers are shown in Table S1. A sample of genotype variability regarding leaf and fruit morphology is shown in Fig. S1.

Seeds were germinated under greenhouse conditions in plastic trays filled with peat-based substrate. In order to ensure seed germination and avoid the spread of fungal and virus diseases, seeds were treated according to the procedure described in Fullana-Pericàs et al. (2019).

2.2. Experimental design and field conditions

The experiment was performed at a commercial tomato field in Ariany (Mallorca, Balearic Islands, latitude 39º38′N, longitude 3º08′E, altitude 79 m a.s.l.) (Fig. 1a). Following commercial procedures, field soil was fumigated at a rate of 300 L ha^{-1} with 50% metam sodium anhydrous (50% p/v) and enriched with 250 kg ha^{-1} of a granulated fertilizer (composition of 12% of total N, 8% of P_2O_5 and 16% of K_2O)

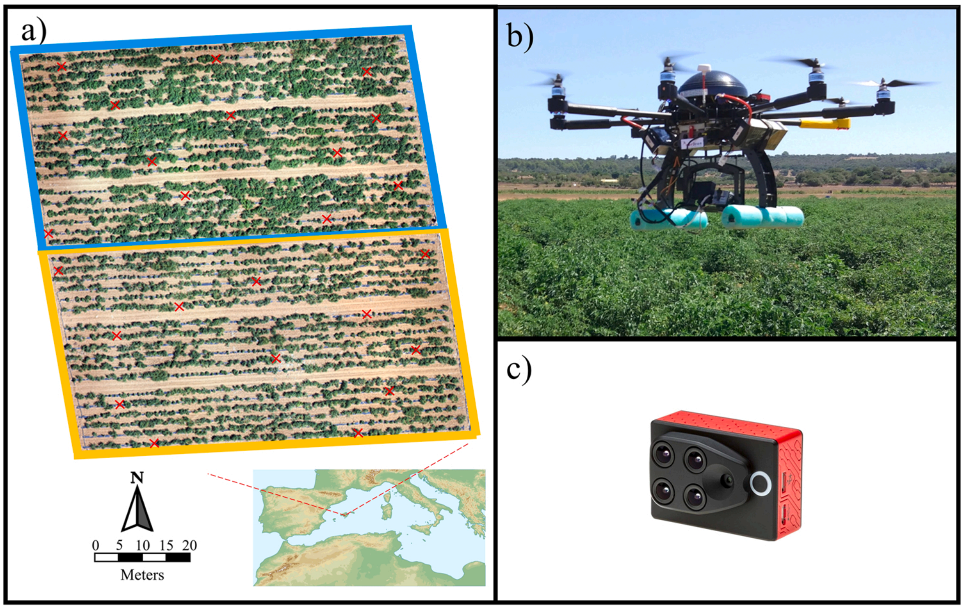

Fig. 1. Images of a) the location of the study (blue square delimits the well-watered treatment and yellow square the water deficit treatment; red crosses indicate the location of the ground control points in the field), b) the UAV (FV8, Atyges, Malaga, Spain) and c) the camera used to obtain the multispectral images (Parrot Sequoia sensor, Parrot SA, Paris, France).

prior transplantation. Field soil was clay and had an electric conductivity of 0.55 mS cm^{-1}, a pH of 8.4. Soil analyses performed before plant transplantation showed low heterogeneity in the main soil parameters (not shown). Outdoor plant beds were 80 m long and 30 cm width, distributed in two blocks separated by 6 m. Plants were irrigated by a black plastic-covered dripping system (AzudPro, 0.33 m emitter spacing, 1 mm thickness, 2.15 L h^{-1} at 100 kPa). Within each block, 5 plants of each genotype were randomly planted one month after germination with a separation of 0.8 m within lines. To avoid differences due to management plants were grown freely, without sustain structures and with no pruning all over the experiment. Pests and weeds were treated following typical commercial practices.

Monthly average temperature (in ºC) and relative air humidity (%) over the experiment were 24.1 and 60 in June, 25.8 and 69 in July, 26.2 and 70 in August, and 20.6 and 76 in September. No rainfall was recorded in June, while 6.0 mm, 8.3 mm and 19.0 mm were registered in July, August, and September, respectively.

2.3. *Irrigation treatments*

Two treatments were stablished, corresponding to each block. Both were irrigated covering the daily crop evapotranspiration (ET_C) during the first month after field transplantation. Afterwards, one block maintained the irrigation covering the daily ET_C (well-watered treatment, WW), while in the other block the irrigation was stopped (water deficit treatment, WD). Thus, over all the cultivation period, WW treatment received 606 mm and WD treatment 215 mm and thus, only ~40% of ETc was covered in WD treatment over the experiment (Fig S2, Table S2).

Weekly reference evapotranspiration was calculated according to FAO-56 (Testa et al., 2011) using data obtained by two nearby weather stations. Crop evapotranspiration (ET_c) was obtained as the product of ET_o and the crop coefficient (K_c) at each growth stage (Allen et al., 2006). The used K_c were: 0.6 for initial, 0.9 for medium and 1.15 for mature and final stages (Table S2). See Fullana-Pericàs et al. (2019) for more details.

2.4. *Leaf gas-exchange and chlorophyll fluorescence*

Leaf gas-exchange and chlorophyll *a* fluorescence were measured 50 days after field transplantation (20 days after WD treatment application) simultaneously with an open infrared gas-exchange analyzer system equipped with a leaf chamber fluorometer (Li-6400–40, Li-Cor Inc., USA). Along the measurements, the vapor pressure deficit (VPD) ranged between 1.1 kPa and 2.8 kPa, with a mean of 2.1 kPa. Measurements were performed from 09:00–14:00 during eight days.

Environmental conditions in the leaf chamber consisted of a photosynthetic photon flux density of 1500 μmol m^{-2} s^{-1} (with 10% blue light), and a leaf temperature of 32 °C. Measurements were performed after inducing steady-state photosynthesis for at least 5 min at an ambient CO_2 concentration (C_a) of 400 μmol CO_2 m^{-2} s^{-1}.

The quantum efficiency of the photosystem II (PSII)-driven electron transport was determined using the Eq. (1):

$$\Phi PSII = \frac{F'_M - F_s}{F'_M} \tag{1}$$

where F_s is the steady-state fluorescence in the light (PPFD 1500 μmol photon m^{-2} s^{-1}) and F'_M the maximum fluorescence obtained with a light-saturating pulse (8500 μmol photon m^{-2} s^{-1}) (Genty et al., 1989). As ΦPSII represents the number of electrons transferred per photon absorbed by PSII, the rate of electron transport (ETR) can be calculated as (2):

$$ETR = \Phi PSII \cdot PPFD \cdot \alpha \cdot \beta \tag{2}$$

where α is the leaf absorbance, and β is the distribution of absorbed energy between the two photosystems. The values of α and β were obtained from Fullana-Pericàs et al. (2017).

2.5. *Leaf $\delta^{13}C$ isotope composition*

Leaf carbon isotope composition ($\delta^{13}C$) was determined from a young fully expanded leaf per plant replicate. Leaves were dried at 60 ºC until constant weight (ca. 72 h), ground to fine powder and sampled for analysis. Samples were combusted in an elemental analyzer (Thermo

Flash EA 1112 Series, Bremen, Germany), and CO_2 and N_2 were directly injected into a continuous-flow isotope ratio mass spectrometer (Thermo-Finnigan Delta XP, Bremen, Germany) for isotope analysis. Peach leaf standards (NIST 1547) were run every six samples. The standard deviation of the analysis was below 0.1‰. Results for $\delta^{13}C$ are presented as δ vs. PDB.

2.6. *Fruit production and quality measurements*

Fruit production was measured at 5 different times, depending on the ripening stage of each genotype. Thus, five different harvests were performed, at 79, 92, 96, 107 and 114 days after field transplantation. In each harvest, only red-ripe fruits (i.e., >90% turned, non-green color, either red or yellow depending on the genotype) were harvested, for any plant of any genotype and treatment. Data shown corresponds to the sum of the five harvests, which was always scored in a per-plant fashion. See Fullana-Pericàs et al. (2019) for more details. For fruit quality, a digital refractometer and electrical conductimeter (PAL-BXACID F5, Atago, Tokyo, Japan) was used to measure the total soluble solids (TSS) and the acidity in 8 healthy fruits per plant.

2.7. *Aerial image analysis*

The images of the study were acquired using an unmanned aerial vehicle (UAV) (FV8, Atyges, Malaga, Spain) (Fig. 1b). The UAV was controlled by an autopilot for autonomous flying (AP04, UAV Navigation, Madrid, Spain) and followed a flight plan using waypoints to acquire imagery from all study field. Aerial measurements were performed 65 days after field transplantation and were performed during the solar noon to avoid plant shadows that could hinder the image analysis.

The UAV was equipped with a Parrot Sequoia sensor (Parrot SA, Paris, France). The Parrot Sequoia sensor imaged with one 16 megapixel rolling shutter RGB camera at 4608 × 3456 pixel resolution and four 1.5 megapixel global-shutter single band cameras imaging at 1280 × 960 pixel resolution in green (550 nm), red (660 nm), red-edge (735 nm) and near infrared (790 nm) spectral bands. Sensors were calibrated by a reflectance panel provided by the manufacturer just before the flight in the takeoff site. This equipment includes a light sensor placed in the top of the UAV that measures the incoming sun radiation during the flight and corrects the reflectance data from the 4 sensors by the fluctuating irradiance. The image resolution (ground pixel size) was of 1.65 cm/pixel at typical established flight altitude of 15 m above the terrain.

The normalized difference vegetation index (NDVI) was calculated as in Rouse et al. (1974):

$$\mathrm{NDVI} = \frac{\mathrm{NIR} - \mathrm{RED}}{\mathrm{NIR} + \mathrm{RED}} \tag{3}$$

Using the same multispectral bands, the simple ratio index (SR) was calculated as:

$$\mathrm{SR} = \frac{\mathrm{NIR}}{\mathrm{RED}} \tag{4}$$

The green normalized difference vegetation index (GNDVI) was calculated using the green band (500–550 mm) as:

$$\mathrm{GNDVI} = \frac{\mathrm{NIR} - \mathrm{GREEN}}{\mathrm{NIR} + \mathrm{GREEN}} \tag{5}$$

Canopy projected area (CPA) was measured using a 16 mm lens RGB camera (Alpha 5000, Sony, Tokyo, Japan) on board measuring the area covered by each plant. The field of view (FOV) was 25.5°, which delivered high-RGB image resolution (ground pixel size) of 0.86 cm/pixel at typical established flight altitude of 30 m above the terrain. Image post-processing was carried out using Pix4DPro (ver. 3.3.29, Pix4D, Lausanne, Switzerland). A total of 25 ground control points (GCPs) were used for geo-referencing of the images using this software. All GCPs were build covering a 20 × 10 cm steel plate with aluminum foil to ease its visualization in images.

Error was assessed using the root-mean-square error (RMSE) of GCPs with values < 0.05 m. Obtained maps were mounted in ArcMap module of ArcGIS (version 10.3.1, ESRI Inc., USA), where individual plant shape was manually extracted. Following this, the different spectral bands were extracted as a mean of the selected region, and multispectral indices were calculated according to the previous formulas. Similarly, CPA was extracted using the individual shapes.

2.8. *Statistical analyses*

One-way ANOVA was performed in all measured parameters to reveal differences between treatments or within treatments for the genotype groups (P-value < 0.05 after Duncan *post-hoc* test). Pearson's correlations (r) were calculated to determine the relationships among the studied parameters. ANCOVA analysis was performed to evaluate differences in intercept and slopes between different regression analyses. All statistical analyses were performed using R software (ver. 3.2.2.; R Core Team, Vienna, Austria).

3. Results

3.1. *Variability in leaf-level physiologic parameters and correlations among them*

Under well-watered (WW) conditions, there were no differences in the net CO_2 assimilation rate (A_N) and stomatal conductance (g_s) between control (CON) and long shelf-life (LSL) genotypes (Table 1). Both CON and LSL had lower A_N and g_s and higher intrinsic water-use efficiency (WUE_i) under water deficit (WD) as compared to WW. However, under WD, average values of LSL for A_N and g_s were ~10% and ~25%, respectively, lower than those of CON. Regarding WUE_i, LSL presented lower average values than CON under WW but higher under WD. Leaf carbon isotope composition ($\delta^{13}C$) values were ~5% higher under the WD than under WW conditions, having the LSL group higher $\delta^{13}C$ average values than CON regardless of the treatment (Table 1).

Concerning the correlations among leaf physiologic measurements, A_N and g_s showed a positive relationship when considering all data, having CON and LSL a similar behavior when considered separately (Fig. 2a). The electron transport rate (ETR) to net CO_2 assimilation rate ratio (ETR/A_N; a physiological indicator of stress) was negatively correlated to g_s (Fig. 2b). Similarly, a negative correlation was found between WUE_i and g_s (Fig. 2c). All these relationships were also significant when considering CON and LSL separately, but ANCOVA analysis did not reveal any difference between such groups in the slope or intercept (P-value > 0.05).

A negative correlation was observed between $\delta^{13}C$ and both A_N and g_s (Fig. 2d,e), with differences between CON and LSL regressions. ANCOVA analysis revealed that LSL had higher A_N and g_s than CON at low $\delta^{13}C$ values. On the contrary, there was a positive relationship between $\delta^{13}C$ and WUE_i when considering all data, although this relationship was only significant for LSL when considering genotype groups separately (Fig. 2f).

3.2. *Variability in remote sensing parameters*

The normalized difference vegetation index (NDVI) and the canopy projected area (CPA) showed similar trends in response to water treatments among genotype groups, having LSL near 5% higher NDVI and 30% CPA values than CON regardless of the treatment (Table 1). Both genotype groups reduced their NDVI and CPA under WD. A significant positive correlation was found between both parameters ($r = 0.59$; P-value < 0.001, Fig. S3).

Table 1

Differences in net CO_2 assimilation rate (A_N), stomatal conductance (g_s), intrinsic water-use efficiency (WUE_i), carbon isotope composition ($\delta^{13}C$), normalized difference vegetation index (NDVI) and canopy projected area (CPA) for the different control (CON) and long shelf-life (LSL) genotype groups under well-watered (WW) and water deficit (WD) conditions. Data are means ± S.E ($n = 23$ for CON and $n = 68$ for LSL). Leaf gas-exchange measurements were performed under saturating light conditions (PAR = 1500 $\mu mol\ m^{-2}s^{-1}$). Letters denote significant differences between groups within treatments and asterisks between treatments for each group by one-way ANOVA after Duncan *post-hoc* test (P-value < 0.05).

	A_N	g_s	WUE_i	$\delta^{13}C$	NDVI	CPA
	$\mu mol\ CO_2\ m^{-2}s^{-1}$	$mol\ H_2O\ m^{-2}s^{-1}$	$\mu mol\ CO_2\ mol^{-1}\ H_2O$	‰		$m^2\ plant^{-1}$
WW						
CON	24.53 ± 0.67^a *	0.55 ± 0.03^a *	53.59 ± 2.53^a *	-28.56 ± 0.01^b *	0.75 ± 0.01^b *	0.97 ± 0.01^b *
LSL	25.21 ± 0.26^a *	0.56 ± 0.01^a *	48.12 ± 0.74^b *	-27.61 ± 0.05^a *	0.78 ± 0.01^a *	1.33 ± 0.01^a *
WD						
CON	18.54 ± 0.80^a	0.31 ± 0.02^a	67.58 ± 2.95^b	-27.49 ± 0.13^b	0.68 ± 0.01^b	0.72 ± 0.01^b
LSL	16.54 ± 0.41^b	0.23 ± 0.01^b	79.74 ± 1.75^a	-26.32 ± 0.06^a	0.72 ± 0.01^a	1.04 ± 0.01^a

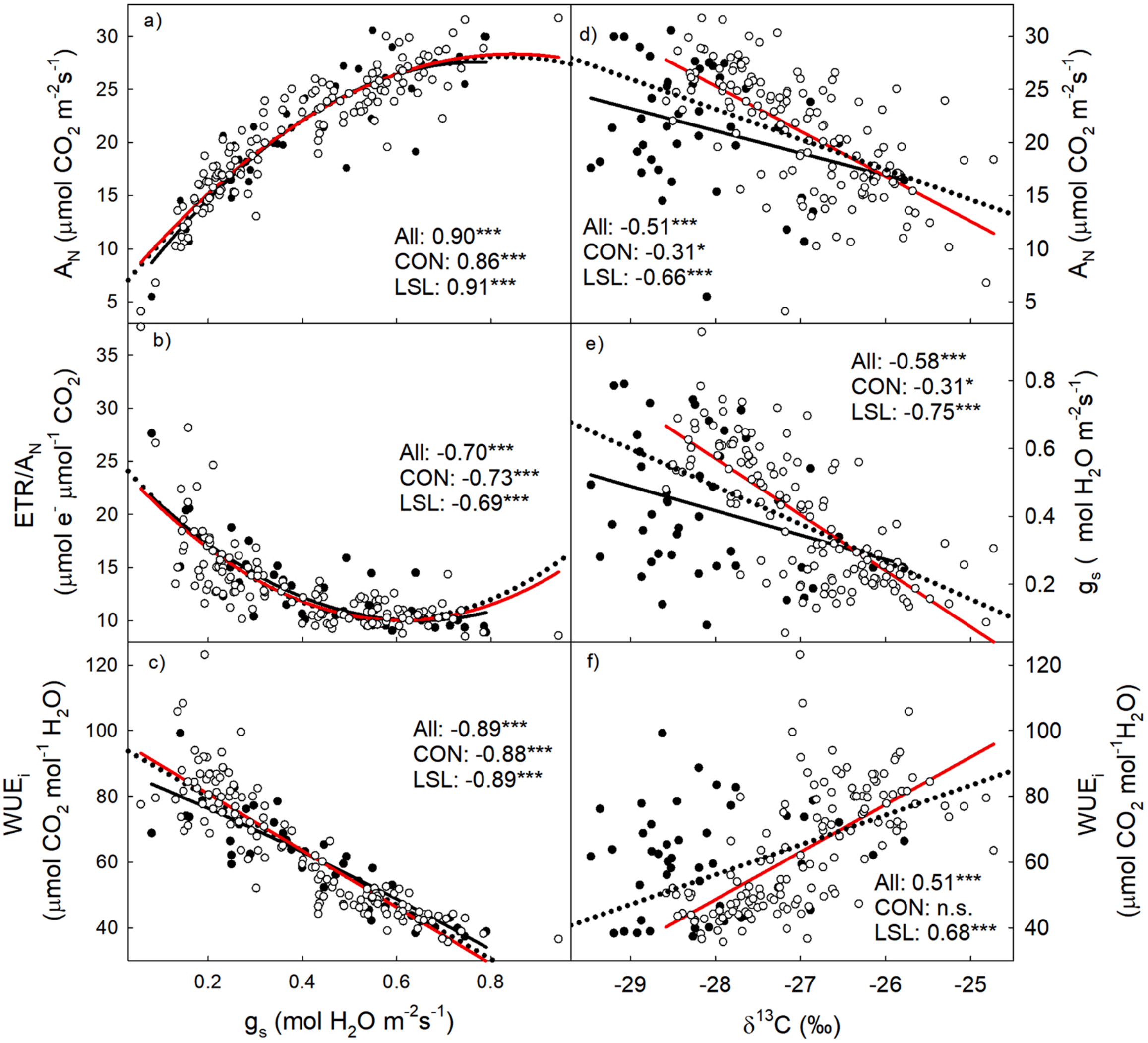

Fig. 2. Relationship between stomatal conductance (g_s) and a) net CO_2 assimilation rate (A_N), b) electron transport rate (ETR) to net CO_2 assimilation rate ratio (ETR/A_N) and c) intrinsic water-use efficiency (WUE_i); and between leaf carbon isotope composition ($\delta^{13}C$) and d) net CO_2 assimilation rate (A_N), e) stomatal conductance (g_s) and f) intrinsic water-use efficiency (WUE_i). Dots refer to genotype mean ($n = 3$–5). Black dots refer to control (CON) and white dots to long shelf-life (LSL) genotypes. Regression lines are shown when significant. In this case dotted black line represents the regression analysis considering all genotypes and treatments, black line the regression analysis considering only CON and red line considering only LSL genotypes. Pearson's correlation coefficient (r) is indicated, and asterisks mean significance level at * $P \leq 0.05$, * * $P \leq 0.01$ or * **$P \leq 0.001$; n.s. refers to non-significant. The best fitting model has always been used and, contrary to the other relationships shown in the study, a) and b) better fit with non-linear models, given the "saturating" nature of such correlations.

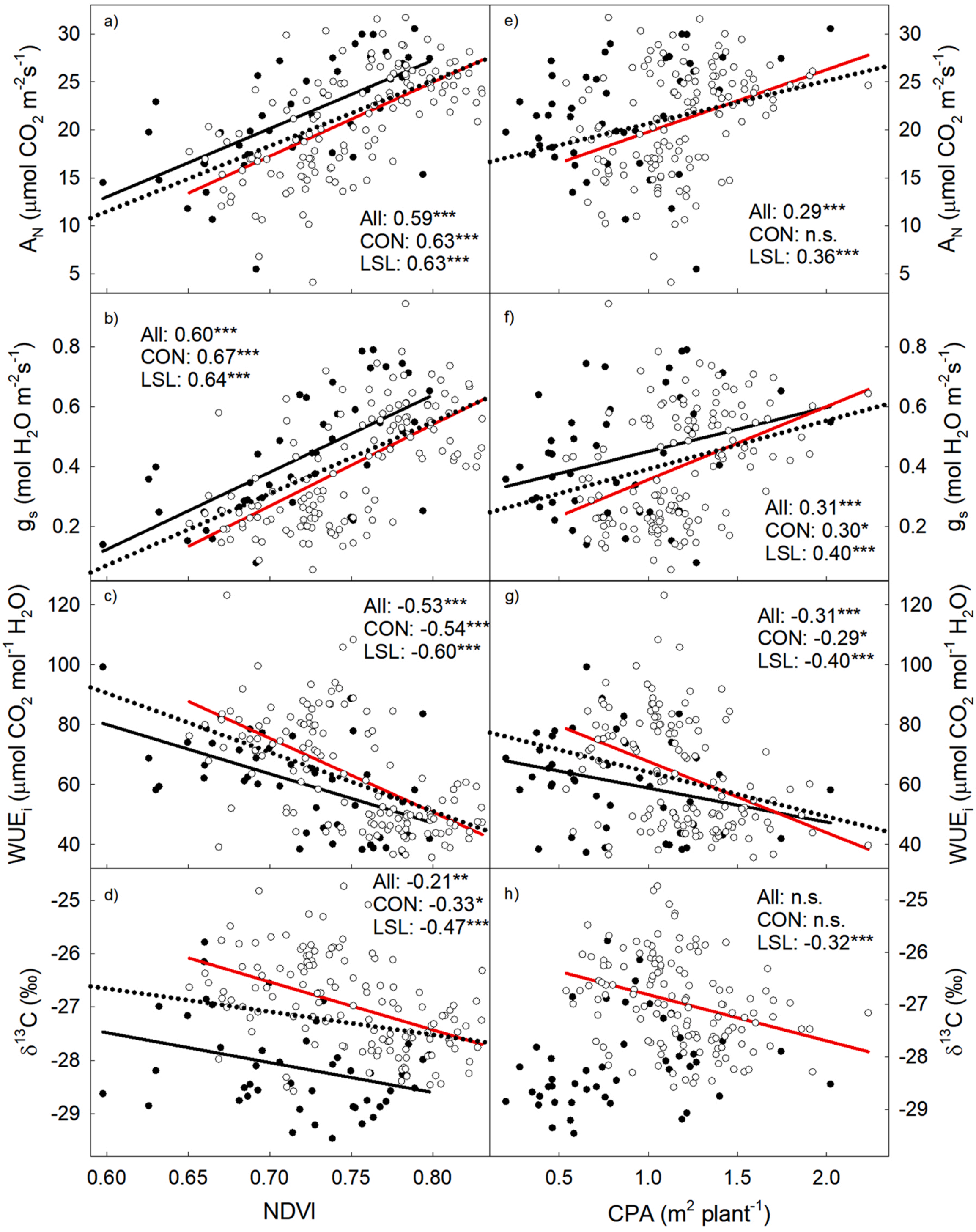

Fig. 3. Relationship between normalized difference visible index (NDVI) and a) net CO_2 assimilation rate (A_N), b) stomatal conductance (g_s), c) intrinsic water-use efficiency (WUE_i) and d) leaf carbon isotope composition ($\delta^{13}C$); and between canopy projected area (CPA) and e) net CO_2 assimilation rate (A_N), f) stomatal conductance (g_s), g) intrinsic water-use efficiency (WUE_i), and h) leaf carbon isotope composition ($\delta^{13}C$). Dots refer to genotype mean (n = 3–5). Black dots refer to control (CON) and white dots to long shelf-life (LSL) genotypes. Regression lines are shown when significant. In this case, dotted black line represents the regression analysis considering all genotypes and treatments, black line the regression analysis considering only CON and red line considering only LSL genotypes. Pearson's correlation coefficient (r) is indicated, and asterisks mean significance level at * $P \leq 0.05$, ** $P \leq 0.01$ or ***$P \leq 0.001$; n.s. refers to non-significant.

3.3. Relationships between leaf-level physiologic and remote sensing measurements

The information obtained through HTPP employing the UAV was compared with the leaf-level physiologic measurements in order to assess their reliability as a high-throughput substitute of plant-level measurements. Contrasting results were obtained when examining the relationship between NDVI and CPA with leaf gas-exchange and carbon isotope composition (Fig. 3). NDVI was positively correlated with both A_N and g_s, either when considering all genotypes and treatments together, and for CON and LSL separately (Fig. 3a,b). Under both water treatments, NDVI was negatively correlated with water use efficiency-related traits, considering either WUE_i and $\delta^{13}C$, for all genotypes together and separately in groups (Fig. 3c,d). For all the relationships previously described, ANCOVA analyses revealed differences between CON and LSL regressions in their intercepts (P-value < 0.05) but not in their slopes.

In general, CPA showed weaker or non-significant relationships with the leaf-level physiologic parameters as compared to the NDVI. Significant correlations with CPA were only observed for A_N, g_s and WUE_i when considering all genotypes together (Fig. 3e,f,g). For CON genotypes, CPA correlated with g_s and WUE_i, while for LSL, significant correlations were found with all leaf-level parameters (Fig. 3e-h). For the correlations with g_s and WUE_i, where both CON and LSL regressions were significant, ANCOVA analysis revealed differences in their intercepts (P-value < 0.05) but not in their slopes.

Other vegetation indexes were obtained from UAV measurements, such as the simple ratio index (SR) and the green normalized difference vegetation index (GNDVI). When considering all genotypes and treatments, both SR and GNDVI correlated with all ground-based parameters (i.e., A_N, g_s, WUE_i and $\delta^{13}C$; Table 2) showing a similar behavior than the previously observed for NDVI.

3.4. Variability in fruit related traits and the relationship with remote sensing parameters

No differences in fruit production were found between LSL and CON, under WW conditions (Table 3). Different to fruit production, there were differences in the total soluble solids (TSS) and acidity between LSL and CON, with higher values in the former group (~10% for TSS and ~30% for acidity). No differences between genotype groups were found for fruit related traits under WD conditions. All genotype groups decreased their fruit production (~30% and ~20% reduction in CON and LSL, respectively) and increased TSS under WD as compared to WW, while only CON increased acidity under WD (Table 3).

The relationships between the UAV remote sensing data and the fruit production and quality parameters was further explored. Fruit production was positively correlated with NDVI either when considering all genotypes and treatments together and considering genotype groups separately (Fig. 4a). Similar regression coefficients resulted for fruit production when correlating it to SR (Fig. 4b) and to GNDVI (Table S3). However, higher correlation coefficients were obtained when fruit production was correlated with CPA (Fig. 4c). Despite NDVI and GNDVI were correlated with TSS when considering all genotypes and treatments (Fig, 4d, Table S3), the correlation of TSS with SR showed higher correlation coefficient and was significant regardless of the genotype group (Fig. 4e). On the other hand, correlation between CPA and TSS was only significant for LSL genotypes (Fig. 4f). Any of the UAV high-throughput parameters was correlated with acidity, except CPA when considering only LSL genotypes (Table S3).

Table 2
Pearson's correlation coefficients (r) between simple ratio (SR) and green normalized difference vegetation index (GNDVI) and ground-based physiologic measurements when considering all genotypes and treatments together (All), only control genotypes (CON) and only long shelf-life genotypes (LSL). Also, the significance level is indicated as: * P-value ≤ 0.05, ** P-value ≤ 0.01 and *** P-value ≤ 0.001.

		A_N	g_s	WUE_i	$\delta^{13}C$
SR	All	0.65***	0.68***	-0.61***	-0.3***
	CON	0.67***	0.73***	-0.59***	-0.35*
	LSL	0.68***	0.7***	-0.66***	-0.52***
GNDVI	All	0.58***	0.58***	-0.51***	-0.17*
	CON	0.62***	0.7***	-0.58***	-0.31*
	LSL	0.61***	0.59***	-0.54***	-0.39***

Table 3
Differences in fruit production, total soluble solids (TSS) and acidity for the different genotype groups under well-watered (WW) and water deficit (WD) conditions. Data are means ± S.E ($n = 23$ for CON and $n = 68$ for LSL). Letters denote significant differences between groups within treatments and asterisks between treatments for each group by one-way ANOVA after Duncan *post-hoc* test (P-value < 0.05).

	Fruit production	TSS	Acidity
	g plant^{-1}	Brix	% citric acid
WW			
CON	3214.7 ± 265.4^{a} *	4.56 ± 0.19^{b} *	0.80 ± 0.07^{b} *
LSL	2886.9 ± 152.4^{a} *	5.01 ± 0.07^{a} *	1.07 ± 0.03^{a}
WD			
CON	2232.6 ± 179.0^{a}	5.92 ± 0.29^{a}	1.08 ± 0.07^{a}
LSL	2276.4 ± 118.1^{a}	5.88 ± 0.10^{a}	1.10 ± 0.03^{a}

4. Discussion

The need for efficient and reliable HTPP methodology is claimed as a major constraint for genetic crop breeding programs (Araus and Kefauver, 2018 and references therein). Despite remote sensing has important advantages related to high automation and reproducibility of measurements over time, the challenge is still the reliability with common leaf-level physiologic parameters or fruit related traits (Araus and Kefauver, 2018; Rötter et al., 2011; Stylinski et al., 2002; Suárez et al., 2008). One of the current pitfalls in most of the studies attempting to correlate remote sensing with those measurements is that include low genetic variability in the screened plant material, which biases the results of the correlation to genotype-related responses (e.g., Duan et al., 2019; Fortes et al., 2015; Wu et al., 2008). The current study, which contains 797 plants from 91 different tomato genotypes, aims to test the usefulness of remote sensing and high-throughput measurements to predict plant stress response in open field tomato crops. The relevance of the study increases given the worldwide importance of the tomato crop, and the ease to transfer results from this model crop to further horticultural, fleshy fruit crops.

4.1. Leaf-level physiologic differences among genotypes are detected with remote sensing measurements

The differences in physiologic parameters between CON and LSL (Table 1) agree with the results reported in previous studies comparing drought adapted LSL genotypes with commercial and non-drought-adapted genotypes, denoting a different physiologic behavior between those groups (Fullana-Pericàs et al., 2019, 2017; Galmés et al., 2013, 2011; Giorio et al., 2018; Guida et al., 2017; Landi et al., 2017; Patanè et al., 2016). In this study, we show that these contrasting performance was also observed at whole-plant level, with differences between CON and LSL in NDVI and CPA regardless of the treatment (Table 1).

Under field conditions, multispectral indices have been related to leaf biochemical parameters such as chlorophyll content and other photosynthetic pigments (Jay et al., 2019; Le Maire et al., 2004; Wu et al., 2008; Zarco-Tejada et al., 2013b). In fact, those indices have been used to track changes in A_N in a processing tomato genotype (Marino et al., 2015) and in corn and orange crops (Tan et al., 2013; Zarco-Tejada et al., 2016, 2013a). The results of the present study, where drought promoted declines in A_N and g_s which were translated in reductions in multispectral indices and CPA (Fig. 3, Table 2), show that remote sensing HTPP parameters are an efficient tool to explore drought impact over the physiologic performance of a large tomato collection.

4.2. Tomato groups presented different regressions between leaf-level and remote sensing measurements

The results of the present experiment corroborate the relationship between physiologic performance and remote sensing in a large tomato

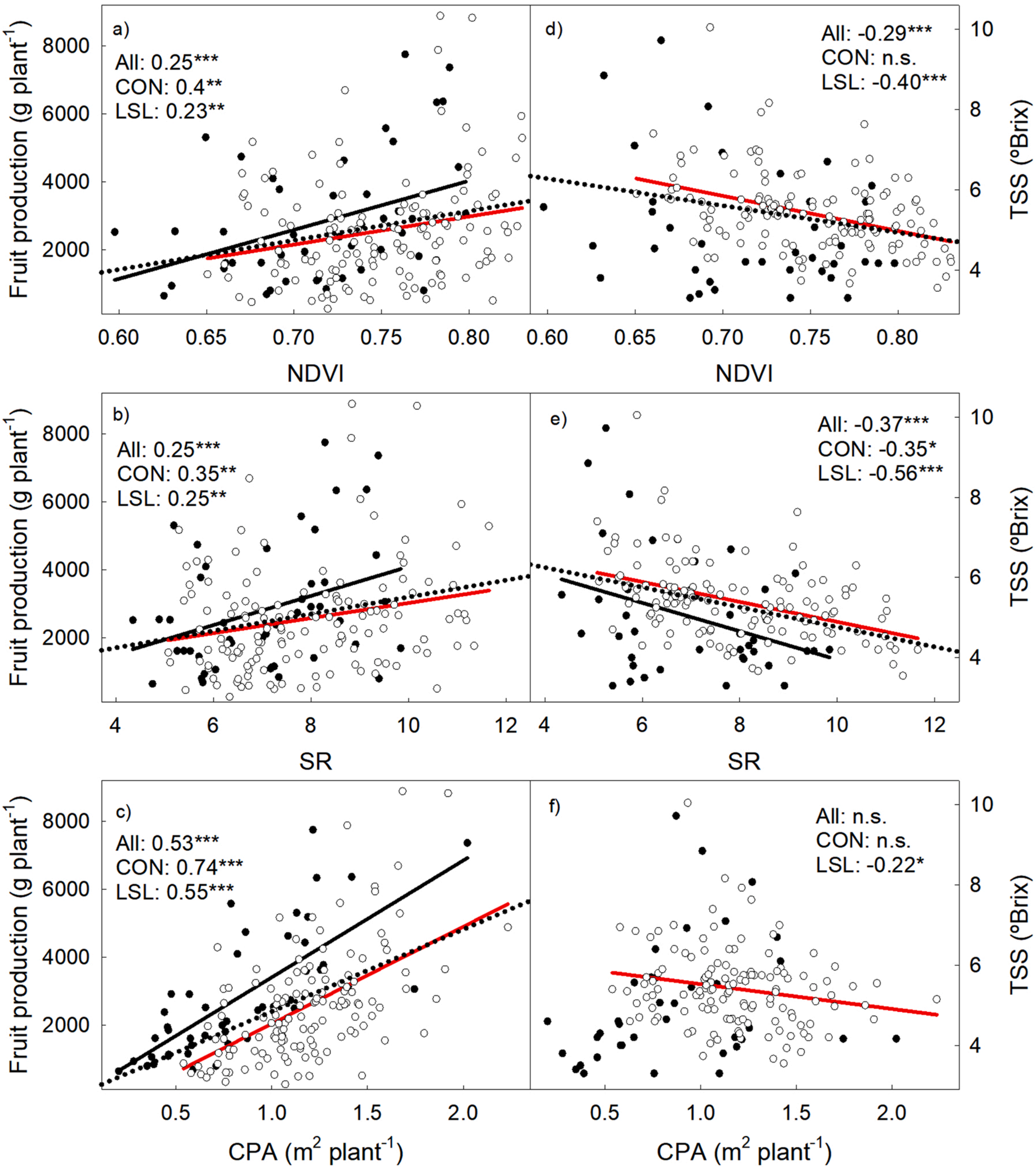

Fig. 4. Relationship between fruit production (g $plant^{-1}$) and a) normalized difference visible index (NDVI), b) simple ratio (SR) and c) canopy projected area (CPA); and between total soluble solids (TSS) and d) normalized difference visible index (NDVI), e) simple ratio (SR) and f) canopy projected area (CPA). Dots refer to genotype mean ($n = 3$–5). Black dots refer to control (CON) and white dots to long shelf-life (LSL) genotypes. Regression lines are shown when significant. In this case, dotted black line represents the regression analysis considering all genotypes and treatments, black line the regression analysis considering only CON and red line considering only LSL genotypes. Pearson's correlation coefficient (r) is indicated, and asterisks mean significance level at $^*P \leq 0.05$, $^{**} P \leq 0.01$ or $^{***}P \leq 0.001$; n.s. refers to non-significant.

collection. Further, ANCOVA analysis revealed different performance of CON and LSL genotypes for these relationships, denoting a different physiologic behavior detected by remote sensing phenotyping. For the same NDVI value, LSL genotypes had lower A_N and g_s than CON (Fig. 3a, b), which in turn lead to larger WUE_i (Fig. 3c). The higher WUE_i of LSL was achieved through a larger reduction in g_s as compared to the reduction in A_N, in accordance with previous reports on tomato landraces with enhanced drought tolerance (Galmés et al., 2013; Giorio et al., 2018; Guida et al., 2017).

Interestingly, CON under WD had similar $\delta^{13}C$ values than LSL under WW, denoting the different behavior in WUE between genotype groups (Table 1). This contrasting performance explains the differences in the relationship of $\delta^{13}C$ with leaf gas-exchange parameters between genotype groups, having LSL higher A_N and g_s than CON for the same $\delta^{13}C$ (Fig. 2d,e), which in turn explains the higher NDVI for LSL genotypes for the same $\delta^{13}C$ values (Fig. 3d).

It is worthy to note that no correlation of CPA with $\delta^{13}C$ was observed for CON, but a negative relationship was found for LSL (Fig. 3i). Several studies related CPA with crop physiologic status, growth, and leaf transpiration (Enciso et al., 2019; Haboudane et al., 2004; Mukherjee et al., 2010). Hence, the higher CPA and lower g_s of LSL as compared to CON under WD indicates that the constrained g_s in LSL (thus, driving higher WUE) do not impose a detriment in plant growth (Table 2).

Aside of the vegetation indices used in this study, plant's temperature directly collected by UAV thermal imagery can be linked to plant water stress by stomata performance and the leaf energy balance (Berni et al., 2009; Gago et al., 2017, 2015). Despite the relationship between leaf temperature and leaf physiology has been explored in tomato (Bhattarai et al., 2021; Camejo et al., 2005; Morales et al., 2003), there is almost no information in literature regarding the use of thermal imagery to monitor changes in physiologic parameters in this crop. Hence, due to the reduced resolution of the microbolometer thermal sensors and its cost, its employment is reduced because of the difficulties to perform adequate high-resolution thermal maps for extended field-trials of herbaceous species that have a reduced canopy compared to trees and vines.

4.3. Fruit production and quality can also be approached using remote sensing measurements in large tomato collections

Fruit production reduction under WD conditions was ~15% lower in LSL than in CON genotypes (Table 3), and the changes in fruit production correlated with remote sensing measurements (Fig. 4a-c). Johansen et al. (2020) used RGB and multispectral indices to develop biomass and fruit production prediction models in a tomato wild species. Other studies have also described correlations between NDVI and tomato fruit production with higher regression coefficients than that obtained in the present study (Campillo et al., 2019; Fortes et al., 2014; Ihuoma and Madramootoo, 2019). As a main difference, previous studies considered only a single genotype in their trials. Our results show that the inclusion of large genotypic variability in phenotyping trials prevents the existence of high correlation coefficients between remote sensing and leaf-level parameters, hindering the obtention of reliable models that could increase HTPP accuracy in tomato crop.

Stronger correlations for fruit production were found with CPA than with multispectral indices (Fig. 4c). The weak correlations between fruit production and multispectral indices (more linked with physiologic traits, Fig. 3) were mostly explained by the low correlation coefficients observed among physiologic and agronomic parameters (Fig. S4). Alternatively, those tomato genotypes with enhanced plant growth and more open canopies (i.e., more exposed zenithally) can sustain higher fruit production. A large intra- and inter-genotypic variability in agronomic, morphologic and quality traits has been described in Mediterranean LSL tomato landraces (Bota et al., 2014; Cebolla-Cornejo et al., 2013; Figàs et al., 2018). In fact, higher correlation coefficients in the relationship between CPA and fruit production were found for CON as compared to LSL (Fig. 4c), indicating that the large variability included in the LSL group was not only agronomical but also in growth behavior.

Beyond the relationship with fruit production, the present study includes, at the best of our knowledge, the first attempt to relate whole-plant remote sensing measurements with tomato fruit quality. In tomato, previous studies related fruit quality with colorimetric and hyperspectral images measured directly on the tomato fruit (Bello et al., 2020; Ramos-Infante et al., 2019). In grapevines and fruit orchards, changes in NDVI plant canopy have been explored as a solution to monitor fruit maturation and estimate fruit quality, with promising results (Meyers et al., 2020; Overbeck et al., 2017; Stagakis et al., 2012; Uribeetxebarria et al., 2019). It has been largely described that tomato plants under water deficit conditions usually present an enhanced fruit quality (i.e., higher TSS and acidity) (reviewed in Beckles, 2012 and Ripoll et al., 2014). In our study, fruit quality traits correlated with the main leaf-level physiologic parameters (Fig. S5) and thus, relationships between fruit quality and multispectral indices should be expected (Fig. 4). Consequently, our results suggest that the use of UAVs equipped with multispectral cameras can be used to monitor both the plant physiologic performance and the fruit TSS in open-field tomato trials.

4.4. Concluding remarks

This research provides crucial information for future HTPP trials, identifying traits and relationships enabling to screen high genotypic variability and its response to WD, as a major constraint for fruit production and fruit quality prediction models from remote sensing data in tomato crop, which could be extended to similar crops. Our results show that leaf physiology and fruit quality traits were better related with multispectral indices as NDVI, GNDVI and SR; whereas fruit production was closely related to CPA. Nevertheless, different correlations were found depending on the genotype group observed. Consequently, UAVs measurements should be mainly considered in phenotyping studies including genotypes with similar physiologic behavior and response to water deficit. In cases where this is not possible or unknown, our outcomes suggest that remote sensing must be combined with plant-based measurements as leaf gas-exchange or leaf δ^{13}C to identify those genotypes with different physiologic behavior, allowing to increase HTPP accuracy.

Declaration of Competing Interest

The authors declare that they have no known competing financial interests or personal relationships that could have appeared to influence the work reported in this paper.

Acknowledgements

We thank to Sergi Boleda, Toni Ribot and Maria Marquès from Agroilla SAT for their technical support and plant agronomic management. Also, to Gerardo Costea, David Alonso, Jaume Canyelles, Joana Maria Fontclara, Xavier Coll, Dr. Cyril Douthe and Dr. Hanan El Aououad for their help in sampling and posterior processing. We are grateful to Drs. Giovanna Attene and Monica Rodríguez (University of Sassari) for providing seeds of the Sardinian accessions. We would also thank to Carlos J. Oliveros (norDrone) for his support regarding the UAV flight campaigns. This research was supported with a pre-doctoral fellowship (FPI/1929/2016) granted by the Government of the Balearic Islands to M. Fullana-Pericàs and by the European Union's Horizon 2020 research and innovation program under the Grant Agreement No. 727929 (TOMRES) awarded to Dr. J. Galmés.

Appendix A. Supporting information

Supplementary data associated with this article can be found in the online version at doi:10.1016/j.agwat.2021.107283.

References

Adão, T., Hruška, J., Pádua, L., Bessa, J., Peres, E., Morais, R., Sousa, J., 2017. Hyperspectral imaging: a review on UAV-based sensors, data processing and applications for agriculture and forestry. Remote Sens. 9, 1110. https://doi.org/10.3390/rs9111110.

Allen, R., Pereira, L.S., Raes, D., Smith, M., 2006. Evapotranspiración del cultivo: Guias para la determinación de los requerimientos de agua de los cultivos. FAO:Estudios FAO Riego y Drenaje 56,, Rome. https://doi.org/10.1590/1983-40632015v4529143.

Araus, J.L., Cairns, J.E., 2014. Field high-throughput phenotyping: the new crop breeding frontier. Trends Plant Sci. 19, 52–61. https://doi.org/10.1016/j.tplants.2013.09.008.

Araus, J.L., Kefauver, S.C., 2018. Breeding to adapt agriculture to climate change: affordable phenotyping solutions. Curr. Opin. Plant Biol. 45, 237–247. https://doi.org/10.1016/j.pbi.2018.05.003.

Araus, J.L., Kefauver, S.C., Zaman-Allah, M., Olsen, M.S., Cairns, J.E., 2018. Translating high-throughput phenotyping into genetic gain. Trends Plant Sci. 23, 451–466. https://doi.org/10.1016/j.tplants.2018.02.001.

Babar, M.A., van Ginkel, M., Klatt, A.R., Prasad, B., Reynolds, M.P., 2006. The potential of using spectral reflectance indices to estimate yield in wheat grown under reduced irrigation. Euphytica 150, 155–172. https://doi.org/10.1007/s10681-006-9104-9.

Battisti, D.S., Naylor, R.L., 2009. Historical warnings of future food insecurity with unprecedented seasonal heat. Sci. (80-.) 323, 240–244. https://doi.org/10.1126/science.1164363.

Beckles, D.M., 2012. Factors affecting the postharvest soluble solids and sugar content of tomato (Solanum lycopersicum L.) fruit. Postharvest Biol. Technol. 63, 129–140. https://doi.org/10.1016/j.postharvbio.2011.05.016.

Bello, T.B., Costa, A.G., da Silva, T.R., Paes, J.L., de Oliveira, M.V.M., 2020. Tomato quality based on colorimetric characteristics of digital images. Rev. Bras. Eng. Agric. e Ambient 24, 567–572. https://doi.org/10.1590/1807-1929/agriambi.v24n8p567-572.

Berni, J., Zarco-Tejada, P.J., Suarez, L., Fereres, E., 2009. Thermal and narrowband multispectral remote sensing for vegetation monitoring from an unmanned aerial vehicle. IEEE Trans. Geosci. Remote Sens. 47, 722–738. https://doi.org/10.1109/TGRS.2008.2010457.

Bhattarai, S., Harvey, J.T., Djidonou, D., Leskovar, D.I., 2021. Exploring morpho-physiological variation for heat stress tolerance in tomato. Plants 10, 1–22. https://doi.org/10.3390/plants10020347.

Bota, J., Conesa, M.À., Ochogavia, J.M., Medrano, H., Francis, D.M., Cifre, J., 2014. Characterization of a landrace collection for Tomàtiga de Ramellet (Solanum lycopersicum L.) from the Balearic Islands. Genet. Resour. Crop Evol. 61, 1131–1146. https://doi.org/10.1007/s10722-014-0096-3.

Cairns, J.E., Sanchez, C., Vargas, M., Ordoñez, R., Araus, J.L., 2012. Dissecting maize productivity: ideotypes associated with grain yield under drought stress and well-watered conditions. J. Integr. Plant Biol. 54, 1007–1020. https://doi.org/10.1111/j.1744-7909.2012.01156.x.

Calderón, R., Navas-Cortés, J.A., Zarco-Tejada, P.J., 2015. Early detection and quantification of verticillium wilt in olive using hyperspectral and thermal imagery over large areas. Remote Sens 7, 5584–5610. https://doi.org/10.3390/rs70505584.

Camejo, D., Rodríguez, P., Morales, M.A., Dell'Amico, J.M., Torrecillas, A., Alarcón, J.J., 2005. High temperature effects on photosynthetic activity of two tomato cultivars with different heat susceptibility. J. Plant Physiol. 162, 281–289. https://doi.org/10.1016/j.jplph.2004.07.014.

Campillo, C., Carrasco, J., Gordillo, J.L., Cordoba, A., Macua, J.I., 2019. Use of satellite images to differentiate productivity zones in commercial processing tomato farms. Acta Hortic. 1233, 97–104. https://doi.org/10.17660/ActaHortic.2019.1233.15.

Caruso, G., Zarco-Tejada, P.J., González-Dugo, V., Moriondo, M., Tozzini, L., Palai, G., Rallo, G., Hornero, A., Primicerio, J., Gucci, R., 2019. High-resolution imagery acquired from an unmanned platform to estimate biophysical and geometrical parameters of olive trees under different irrigation regimes. PLoS One 14, 1–19. https://doi.org/10.1371/journal.pone.0210804.

Casals, J., Pascual, L., Cañizares, J., Cebolla-Cornejo, J., Casañas, F., Nuez, F., 2012. Genetic basis of long shelf life and variability into Penjar tomato. Genet. Resour. Crop Evol. 59, 219–229. https://doi.org/10.1007/s10722-011-9677-6.

Cebolla-Cornejo, J., Roselló, S., Nuez, F., 2013. Phenotypic and genetic diversity of Spanish tomato landraces. Sci. Hortic. (Amst.) 162, 150–164. https://doi.org/10.1016/j.scienta.2013.07.044.

Comar, A., Burger, P., de Solan, B., Baret, F., Daumard, F., Hanocq, J.-F., 2012. A semi-automatic system for high throughput phenotyping wheat cultivars in-field conditions: description and first results. Funct. Plant Biol. 39, 914–924. https://doi.org/10.1071/FP12065.

Condon, A., Richards, R., Rebetzke, G., Farguhar, G., 2002. Improving Intrinsic water-use efficiency and crop yield. Crop Sci. 42, 122–131.

Condon, A.G., 2004. Breeding for high water-use efficiency. J. Exp. Bot. 55, 2447–2460. https://doi.org/10.1093/jxb/erh277.

Conesa, M. a, Galmés, J., Ochogavía, J.M., March, J., Jaume, J., Martorell, A., Francis, D. M., Medrano, H., Rose, J.K.C., Cifre, J., 2014. The postharvest tomato fruit quality of long shelf-life Mediterranean landraces is substantially influenced by irrigation regimes. Postharvest Biol. Technol. 93, 11–121. https://doi.org/10.1016/j.postharvbio.2014.02.014.

Conesa, M.À., Fullana-Pericàs, M., Granell, A., Galmés, J., 2020. Mediterranean long shelf-life landraces: an untapped genetic resource for tomato Improvement. Front. Plant Sci. 10, 1–21. https://doi.org/10.3389/fpls.2019.01651.

Cuartero, J., Fernández-Muñoz, R., 1999. Tomato and salinity. Sci. Hortic. (Amst.). 78, 83–125.

Daniel, I.O., Atinsola, K.O., Ajala, M.O., Popoola, A.R., 2016. Phenotyping a tomato breeding population by manual field evaluation and digital imaging analysis. Int. J. Plant Breed. Genet. 11, 19–24. https://doi.org/10.3923/ijpbg.2017.19.24.

Dhanapal, A.P., Ray, J.D., Singh, S.K., Hoyos-Villegas, V., Smith, J.R., Purcell, L.C., Andy King, C., Cregan, P.B., Song, Q., Fritschi, F.B., 2015. Genome-wide association study (GWAS) of carbon isotope ratio (δ13C) in diverse soybean [Glycine max (L.) Merr.] genotypes. Theor. Appl. Genet. 128, 73–91. https://doi.org/10.1007/s00122-014-2413-9.

Duan, B., Fang, S., Zhu, R., Wu, X., Wang, S., Gong, Y., Peng, Y., 2019. Remote estimation of rice yield with unmanned aerial vehicle (UAV) data and spectral mixture analysis. Front. Plant Sci. 10, 1–14. https://doi.org/10.3389/fpls.2019.00204.

Eamus, D., 1991. The interaction of rising CO_2 and temperatures with water use efficiency. Plant, Cell Environ. 14, 843–852. https://doi.org/10.1111/j.1365-3040.1991.tb01447.x.

Enciso, J., Avila, C.A., Jung, J., Elsayed-Farag, S., Chang, A., Yeom, J., Landivar, J., Maeda, M., Chavez, J.C., 2019. Validation of agronomic UAV and field measurements for tomato varieties. Comput. Electron. Agric. 158, 278–283. https://doi.org/10.1016/j.compag.2019.02.011.

FAO [WWW Document], 2021. URL ⟨http://www.fao.org/faostat⟩ (accessed 7.1.19).

Farquhar, G.D., Richards, R.A., 1984. Isotopic composition of plant carbon correlates with water-use efficiency of wheat genotypes. Aust. J. Plant Physiol. 11, 539–552. https://doi.org/10.1071/PP9840539.

Figàs, M.R., Prohens, J., Casanova, C., Fernández-de-Córdova, P., Soler, S., 2018. Variation of morphological descriptors for the evaluation of tomato germplasm and their stability across different growing conditions. Sci. Hortic. (Amst.) 238, 107–115. https://doi.org/10.1016/j.scienta.2018.04.039.

Flanagan, L.B., Farquhar, G.D., 2014. Variation in the carbon and oxygen isotope composition of plant biomass and its relationship to water-use efficiency at the leaf- and ecosystem-scales in a northern Great Plains grassland. Plant. Cell Environ. 37, 425–438. https://doi.org/10.1111/pce.12165.

Flexas, J., Medrano, H., 2002. Drought-inhibition of photosynthesis in C3 plants: Stomatal and non-stomatal limitations revisited. Ann. Bot. 89, 183–189. https://doi.org/10.1093/aob/mcf027.

Fortes, R., Prieto, M.H., Blanco, J., Campillo, C., 2014. Using apparent electric conductivity and NDVI measurements for yield estimation of processing tomato crop. Trans. ASABE 57, 827–835. https://doi.org/10.13031/trans.57.10456.

Fortes, R., Prieto, M.H., García-Martín, A., Córdoba, A., Martínez, L., Campillo, C., 2015. Using NDVI and guided sampling to develop yield prediction maps of processing tomato crop. Span. J. Agric. Res. 13, 1–9. https://doi.org/10.5424/sjar/2015131-6532.

Fullana-Pericàs, M., Conesa, M.À., Douthe, C., El Aou-ouad, H., Ribas-Carbó, M., Galmés, J., 2019. Tomato landraces as a source to minimize yield losses and improve fruit quality under water deficit conditions. Agric. Water Manag. 223, 105722 https://doi.org/10.1016/j.agwat.2019.105722.

Fullana-Pericàs, M., Conesa, M.À., Soler, S., Ribas-Carbó, M., Granell, A., Galmés, J., 2017. Variations of leaf morphology, photosynthetic traits and water-use efficiency in Western-Mediterranean tomato landraces. Photosynthetica 55, 121–133. https://doi.org/10.1007/s11099-016-0653-4.

Gago, J., Douthe, C., Coopman, R.E., Gallego, P.P., Ribas-Carbo, M., Flexas, J., Escalona, J., Medrano, H., 2015. UAVs challenge to assess water stress for sustainable agriculture. Agric. Water Manag. 153, 9–19. https://doi.org/10.1016/j.agwat.2015.01.020.

Gago, J., Fernie, A.R., Nikoloski, Z., Tohge, T., Martorell, S., Escalona, J.M., Ribas-Carbó, M., Flexas, J., Medrano, H., 2017. Integrative field scale phenotyping for investigating metabolic components of water stress within a vineyard. Plant Methods 13, 90. https://doi.org/10.1186/s13007-017-0241-z.

Galmés, J., Conesa, M.A., Ochogavía, J.M., Perdomo, J.A., Francis, D.M., Ribas-Carbó, M., Savé, R., Flexas, J., Medrano, H., Cifre, J., 2011. Physiological and morphological adaptations in relation to water use efficiency in Mediterranean accessions of Solanum lycopersicum. Plant, Cell Environ. 34, 245–260. https://doi.org/10.1111/j.1365-3040.2010.02239.x.

Galmés, J., Ochogavía, J.M., Gago, J., Roldán, E.J., Cifre, J., Conesa, M.À., 2013. Leaf responses to drought stress in Mediterranean accessions of Solanum lycopersicum: anatomical adaptations in relation to gas exchange parameters. Plant, Cell Environ. 36, 920–935. https://doi.org/10.1111/pce.12022.

Gamon, J.A., Kovalchuck, O., Wong, C.Y.S., Harris, A., Garrity, S.R., 2015. Monitoring seasonal and diurnal changes in photosynthetic pigments with automated PRI and NDVI sensors. Biogeosciences 12, 4149–4159. https://doi.org/10.5194/bg-12-4149-2015.

Genty, B., Briantais, J.-M., Baker, N.R., 1989. The relationship between the quantum yield of photosynthetic electron transport and quenching of chlorophyll fluorescence. Biochim. Biophys. Acta - Gen. Subj. 990, 87–92. https://doi.org/10.1016/S0304-4165(89)80016-9.

Gianquinto, G., Orsini, F., Fecondini, M., Mezzetti, M., Sambo, P., Bona, S., 2011. A methodological approach for defining spectral indices for assessing tomato nitrogen status and yield. Eur. J. Agron. 35, 135–143. https://doi.org/10.1016/j.eja.2011.05.005.

Giorgi, F., Lionello, P., 2008. Climate change projections for the Mediterranean region. Glob. Planet. Change 63, 90–104. https://doi.org/10.1016/j.gloplacha.2007.09.005.

Giorio, P., Guida, G., Mistretta, C., Sellami, M.H., Oliva, M., Punzo, P., Iovieno, P., Arena, C., De Maio, A., Grillo, S., Albrizio, R., 2018. Physiological, biochemical and molecular responses to water stress and rehydration in Mediterranean adapted tomato landraces. Plant Biol. 20, 995–1004. https://doi.org/10.1111/plb.12891.

Giovannoni, J.J., 2006. Breeding new life into plant metabolism. Nat. Biotechnol. 24, 418–419. https://doi.org/10.1038/nbt0406-418.

Goel, P., Prasher, S., Landry, J., Patel, R., Bonnell, R., Viau, A., Miller, J., 2003. Potential of airborne hyperspectral remote sensing to detect nitrogen deficiency and weed infestation in corn. Comput. Electron. Agric. 38, 99–124. https://doi.org/10.1016/S0168-1699(02)00138-2.

Guida, G., Sellami, M.H., Mistretta, C., Oliva, M., Buonomo, R., De Mascellis, R., Patanè, C., Rouphael, Y., Albrizio, R., Giorio, P., 2017. Agronomical, physiological and fruit quality responses of two Italian long-storage tomato landraces under rain-fed and full irrigation conditions. Agric. Water Manag. 180, 126–135. https://doi.org/10.1016/j.agwat.2016.11.004.

Haboudane, D., Miller, J.R., Pattey, E., Zarco-Tejada, P.J., Strachan, I.B., 2004. Hyperspectral vegetation indices and novel algorithms for predicting green LAI of crop canopies: Modeling and validation in the context of precision agriculture. Remote Sens. Environ. 90, 337–352. https://doi.org/10.1016/j.rse.2003.12.013.

Harmanto, Salokhe, Babel, V.M., Tantau, M.S., H.J, 2005. Water requirement of drip irrigated tomatoes grown in greenhouse in tropical environment. Agric. Water Manag. 71, 225–242. https://doi.org/10.1016/j.agwat.2004.09.003.

Hertig, E., Tramblay, Y., 2017. Regional downscaling of Mediterranean droughts under past and future climatic conditions. Glob. Planet. Change 151, 36–48. https://doi.org/10.1016/j.gloplacha.2016.10.015.

Ihuoma, S.O., Madramootoo, C.A., 2019. Sensitivity of spectral vegetation indices for monitoring water stress in tomato plants. Comput. Electron. Agric. 163, 104860 https://doi.org/10.1016/j.compag.2019.104860.

Janni, M., Coppede, N., Bettelli, M., Briglia, N., Petrozza, A., Summerer, S., Vurro, F., Danzi, D., Cellini, F., Marmiroli, N., Pignone, D., Iannotta, S., Zappettini, A., 2019. In vivo phenotyping for the early detection of drought stress in tomato. Plant Phenomics 2019, 2019. https://doi.org/10.34133/2019/6168209.

Jay, S., Baret, F., Dutartre, D., Malatesta, G., Héno, S., Comar, A., Weiss, M., Maupas, F., 2019. Exploiting the centimeter resolution of UAV multispectral imagery to improve remote-sensing estimates of canopy structure and biochemistry in sugar beet crops. Remote Sens. Environ. 231, 110898 https://doi.org/10.1016/j.rse.2018.09.011.

Johansen, K., Morton, M.J.L., Malbeteau, Y., Aragon, B., Al-Mashharawi, S., Ziliani, M. G., Angel, Y., Fiene, G., Negrão, S., Mousa, M.A.A., Tester, M.A., McCabe, M.F., 2020. Predicting biomass and yield in a tomato phenotyping experiment using UAV imagery and random forest. Front. Artif. Intell. 3, 3. https://doi.org/10.3389/frai.2020.00028.

Johansen, K., Morton, M.J.L., Malbeteau, Y.M., Aragon, B., Al-Mashharawi, S.K., Ziliani, M.G., Angel, Y., Fiene, G.M., Negrão, S.S.C., Mousa, M.A.A., Tester, M.A., McCabe, M.F., 2019. Unmanned aerial vehicle-based phenotyping using morphometric and spectral analysis can quantify responses of wild tomato plants to salinity stress. Front. Plant Sci. 10, 1–18. https://doi.org/10.3389/fpls.2019.00370.

Klee, H.J., Giovannoni, J.J., 2011. Genetics and control of tomato fruit ripening and quality attributes. Annu. Rev. Genet. 45, 41–59. https://doi.org/10.1146/annurev-genet-110410-132507.

Landi, S., De Lillo, A., Nurcato, R., Grillo, S., Esposito, S., 2017. In-field study on traditional Italian tomato landraces: the constitutive activation of the ROS scavenging machinery reduces effects of drought stress. Plant Physiol. Biochem. 118, 150–160. https://doi.org/10.1016/j.plaphy.2017.06.011.

Le Maire, G., François, C., Dufrêne, E., 2004. Towards universal broad leaf chlorophyll indices using PROSPECT simulated database and hyperspectral reflectance measurements. Remote Sens. Environ. 89, 1–28. https://doi.org/10.1016/j.rse.2003.09.004.

Marino, S., Cocozza, C., Tognetti, R., Alvino, A., 2015. Use of proximal sensing and vegetation indexes to detect the inefficient spatial allocation of drip irrigation in a spot area of tomato field crop. Precis. Agric. 16, 613–629. https://doi.org/10.1007/s11119-015-9396-7.

Medrano, H., Tomás, M., Martorell, S., Flexas, J., Hernández, E., Rosselló, J., Pou, A., Escalona, J.M., Bota, J., 2015. From leaf to whole-plant water use efficiency (WUE) in complex canopies: limitations of leaf WUE as a selection target. Crop J. 3, 220–228. https://doi.org/10.1016/j.cj.2015.04.002.

Meyers, J.M., Dokoozlian, N., Ryan, C., Bioni, C., Vanden Heuvel, J.E., 2020. A new, satellite NDVI-based sampling protocol for grape maturation monitoring. Remote Sens 12, 1159. https://doi.org/10.3390/rs12071159.

Mickelbart, M.V., Hasegawa, P.M., Bailey-Serres, J., 2015. Genetic mechanisms of abiotic stress tolerance that translate to crop yield stability. Nat. Rev. Genet. 16, 237–251. https://doi.org/10.1038/nrg3901.

Morales, D., Rodríguez, P., Dell'Amico, J., Nicolás, E., Torrecillas, A., Sánchez-Blanco, M. J., 2003. High-temperature preconditioning and thermal shock imposition affects water relations, gas exchange and root hydraulic conductivity in tomato. Biol. Plant. 46, 203–208. https://doi.org/10.1023/B:BIOP.0000022252.70836.fc.

Mukherjee, A., Kundu, M., Sarkar, S., 2010. Role of irrigation and mulch on yield, evapotranspiration rate and water use pattern of tomato (Lycopersicon esculentum L.). Agric. Water Manag. 98, 182–189. https://doi.org/10.1016/j.agwat.2010.08.018.

Ochogavía, J.M., López, M., Rigo, M., Garau, M., March, J., Moscardó, J., Jaume, J., Conesa, M.À., Galmés, J., Bota, J., Francis, D., Medrano, H., Martorell, A., Cifre, J., 2011.Caracterització de les poblacions de tomàtiga de ramellet de les Illes Balears.

Overbeck, V., Schmitz, M., Blanke, M., 2017. Non-destructive sensor-based prediction of maturity and optimum harvest date of sweet cherry fruit. Sens. (Switz.) 17, 1–12. https://doi.org/10.3390/s17020277.

Padilla, F.M., Peña-Fleitas, M.T., Gallardo, M., Thompson, R.B., 2015. Threshold values of canopy reflectance indices and chlorophyll meter readings for optimal nitrogen nutrition of tomato. Ann. Appl. Biol. 166, 271–285. https://doi.org/10.1111/aab.12181.

Patanè, C., Scordia, D., Testa, G., Cosentino, S.L., 2016. Physiological screening for drought tolerance in Mediterranean long-storage tomato. Plant Sci. 249, 25–34. https://doi.org/10.1016/j.plantsci.2016.05.006.

Ramos-Infante, S.J., Suarez-Rubio, V., Luri-Esplandiu, P., Saiz-Abajo, M.J., 2019. Assessment of Tomato Quality Characteristics Using Vis/Nir Hyperspectral Imaging and Chemometrics. In: Workshop on Hyperspectral Image and Signal Processing, Evolution in Remote Sensing. IEEE, pp. 1–5. https://doi.org/10.1109/WHISPERS.2019.8921170.

Raymond, F., Ullmann, A., Tramblay, Y., Drobinski, P., Camberlin, P., 2019. Evolution of Mediterranean extreme dry spells during the wet season under climate change. Reg. Environ. Chang. 19, 2339–2351. https://doi.org/10.1007/s10113-019-01526-3.

Ripoll, J., Urban, L., Staudt, M., Lopez-Lauri, F., Bidel, L.P.R., Bertin, N., 2014. Water shortage and quality of fleshy fruits-making the most of the unavoidable. J. Exp. Bot. 65, 4097–4117. https://doi.org/10.1093/jxb/eru197.

Rötter, R.P., Carter, T.R., Olesen, J.E., Porter, J.R., 2011. Crop-climate models need an overhaul. Nat. Clim. Chang. 1, 175–177. https://doi.org/10.1038/nclimate1152.

Rouse, R.W.H., Haas, J.A.W., Deering, D.W., 1974. Monitoring Vegetation Systems in the Great Plains with ERTS. In: Third Earth Resources Technology Satellite-1 Symposium- Volume I: Technical Presentations. NASA SP-351, pp. 309–317.

Sacco, A., Cammareri, M., Vitiello, A., Palombieri, S., Riccardi, R., Spigno, P., Grandillo, S., 2017. Italian traditional tomato varieties: a focus on the campania region, in: I Congrés de La Tomaca Valenciana: La Tomaca Valenciana d'El Perelló. pp. 179–193. doi:10.4995/TOMAVAL2017.2017.6526.

Salas Fernandez, M.G., Bao, Y., Tang, L., Schnable, P.S., 2017. A high-throughput, field-based phenotyping technology for tall biomass crops. Plant Physiol. 174, 2008–2022. https://doi.org/10.1104/pp.17.00707.

Sinesio, F., Moneta, E., Peparaio, M., 2007. Sensory characteristics of traditional field grown tomato genotypes in Southern Italy. J. Food Qual. 30, 878–895. https://doi.org/10.1111/j.1745-4557.2007.00161.x.

Stagakis, S., González-Dugo, V., Cid, P., Guillén-Climent, M.L., Zarco-Tejada, P.J., 2012. Monitoring water stress and fruit quality in an orange orchard under regulated deficit irrigation using narrow-band structural and physiological remote sensing indices. ISPRS J. Photogramm. Remote Sens. 71, 47–61. https://doi.org/10.1016/j.isprsjprs.2012.05.003.

Steltzer, H., Welker, J.M., 2006. Modeling the effect of photosynthetic vegetation properties on the NDVI–LAI relationship. Ecology 87, 2765–2772. https://doi.org/10.1890/0012-9658(2006)87[2765:MTEOPV]2.0.CO;2.

Stylinski, C.D., Gamon, J.A., Oechel, W.C., 2002. Seasonal patterns of reflectance indices, carotenoid pigments and photosynthesis of evergreen chaparral species. Oecologia 131, 366–374. https://doi.org/10.1007/s00442-002-0905-9.

Suárez, L., Zarco-Tejada, P.J., Sepulcre-Cantó, G., Pérez-Priego, O., Miller, J.R., Jiménez-Muñoz, J.C., Sobrino, J., 2008. Assessing canopy PRI for water stress detection with diurnal airborne imagery. Remote Sens. Environ. 112, 560–575. https://doi.org/10.1016/j.rse.2007.05.009.

Tambussi, E.A., Bort, J., Araus, J.L., 2007. Water use efficiency in C 3 cereals under Mediterranean conditions: a review of physiological aspects. Ann. Appl. Biol. 150, 307–321. https://doi.org/10.1111/j.1744-7348.2007.00143.x.

Tan, C., Samanta, A., Jin, X., Tong, L., Ma, C., Guo, W., Knyazikhin, Y., Myneni, R.B., 2013. Using hyperspectral vegetation indices to estimate the fraction of photosynthetically active radiation absorbed by corn canopies. Int. J. Remote Sens. 34, 8789–8802. https://doi.org/10.1080/01431161.2013.853143.

Terzopoulos, P.J., Bebeli, P.J., 2010. Phenotypic diversity in Greek tomato (Solanum lycopersicum L.) landraces. Sci. Hortic. (Amst.) 126, 138–144. https://doi.org/10.1016/j.scienta.2010.06.022.

Testa, G., Gresta, F., Cosentino, S.L., 2011. Dry matter and qualitative characteristics of alfalfa as affected by harvest times and soil water content. Eur. J. Agron. 34, 144–152. https://doi.org/10.1016/j.eja.2010.12.001.

The Tomato Genome Consortium, 2012. The tomato genome sequence provides insights into fleshy fruit evolution. Nature 485, 635–641. https://doi.org/10.1038/nature11119.

Tranchida-Lombardo, V., Mercati, F., Avino, M., Punzo, P., Fiore, M.C., Poma, I., Patanè, C., Guarracino, M.R., Sunseri, F., Tucci, M., Grillo, S., 2018. Genetic diversity in a collection of Italian long storage tomato landraces as revealed by SNP markers array. Plant Biosyst. - Int. J. Deal. all Asp. Plant Biol. 3504, 1–10. https://doi.org/10.1080/11263504.2018.1478900.

Uribeetxebarria, A., Martínez-Casasnovas, J.A., Escolà, A., Rosell-Polo, J.R., Arnó, J., 2019. Stratified sampling in fruit orchards using cluster-based ancillary information maps: a comparative analysis to improve yield and quality estimates. Precis. Agric. 20, 179–192. https://doi.org/10.1007/s11119-018-9619-9.

Virlet, N., Costes, E., Martinez, S., Kelner, J.J., Regnard, J.L., 2015. Multispectral airborne imagery in the field reveals genetic determinisms of morphological and transpiration traits of an apple tree hybrid population in response to water deficit. J. Exp. Bot. 66, 5453–5465. https://doi.org/10.1093/jxb/erv355.

Vuong, V., Slaughter, D.C., Roo, C., Clair St., D., Kubond, B., Bosland, P., 2020. In-field high-throughput phenotyping approach using a multi-view and multi-sensor ground-based vehicle (Conference Presentation). In: Thomasson, J.A., Torres-Rua, A.F. (Eds.), Autonomous Air and Ground Sensing Systems for Agricultural Optimization and Phenotyping V. SPIE.

Wu, C., Niu, Z., Tang, Q., Huang, W., 2008. Estimating chlorophyll content from hyperspectral vegetation indices: Modeling and validation. Agric. . Meteorol. 148, 1230–1241. https://doi.org/10.1016/j.agrformet.2008.03.005.

Zarco-Tejada, P.J., Berjón, A., López-Lozano, R., Miller, J.R., Martín, P., Cachorro, V., González, M.R., De Frutos, A., 2005. Assessing vineyard condition with hyperspectral indices: leaf and canopy reflectance simulation in a row-structured discontinuous canopy. Remote Sens. Environ. 99, 271–287. https://doi.org/10.1016/j.rse.2005.09.002.

Zarco-Tejada, P.J., Catalina, A., González, M.R., Martín, P., 2013a. Relationships between net photosynthesis and steady-state chlorophyll fluorescence retrieved from airborne hyperspectral imagery. Remote Sens. Environ. 136, 247–258. https://doi.org/10.1016/j.rse.2013.05.011.

Zarco-Tejada, P.J., González-Dugo, V., Berni, J.A.J., 2012. Fluorescence, temperature and narrow-band indices acquired from a UAV platform for water stress detection using a micro-hyperspectral imager and a thermal camera. Remote Sens. Environ. 117, 322–337. https://doi.org/10.1016/j.rse.2011.10.007.

Zarco-Tejada, P.J., González-Dugo, M.V., Fereres, E., 2016. Seasonal stability of chlorophyll fluorescence quantified from airborne hyperspectral imagery as an indicator of net photosynthesis in the context of precision agriculture. Remote Sens. Environ. 179, 89–103. https://doi.org/10.1016/j.rse.2016.03.024.

Zarco-Tejada, P.J., Guillén-Climent, M.L., Hernández-Clemente, R., Catalina, A., González, M.R., Martín, P., 2013b. Estimating leaf carotenoid content in vineyards using high resolution hyperspectral imagery acquired from an unmanned aerial vehicle (UAV). Agric. . Meteorol. 171–172, 281–294. https://doi.org/10.1016/j.agrformet.2012.12.013.